中国科学院大学
University of Chinese Academy of Sciences

ICTP-AP
International Centre
for Theoretical Physics Asia-Pacific
国际理论物理中心-亚太地区

Probing Inflationary Origins of Primordial Black Holes with LIGO–Virgo–KAGRA O1–O4a data

Mai Qiao

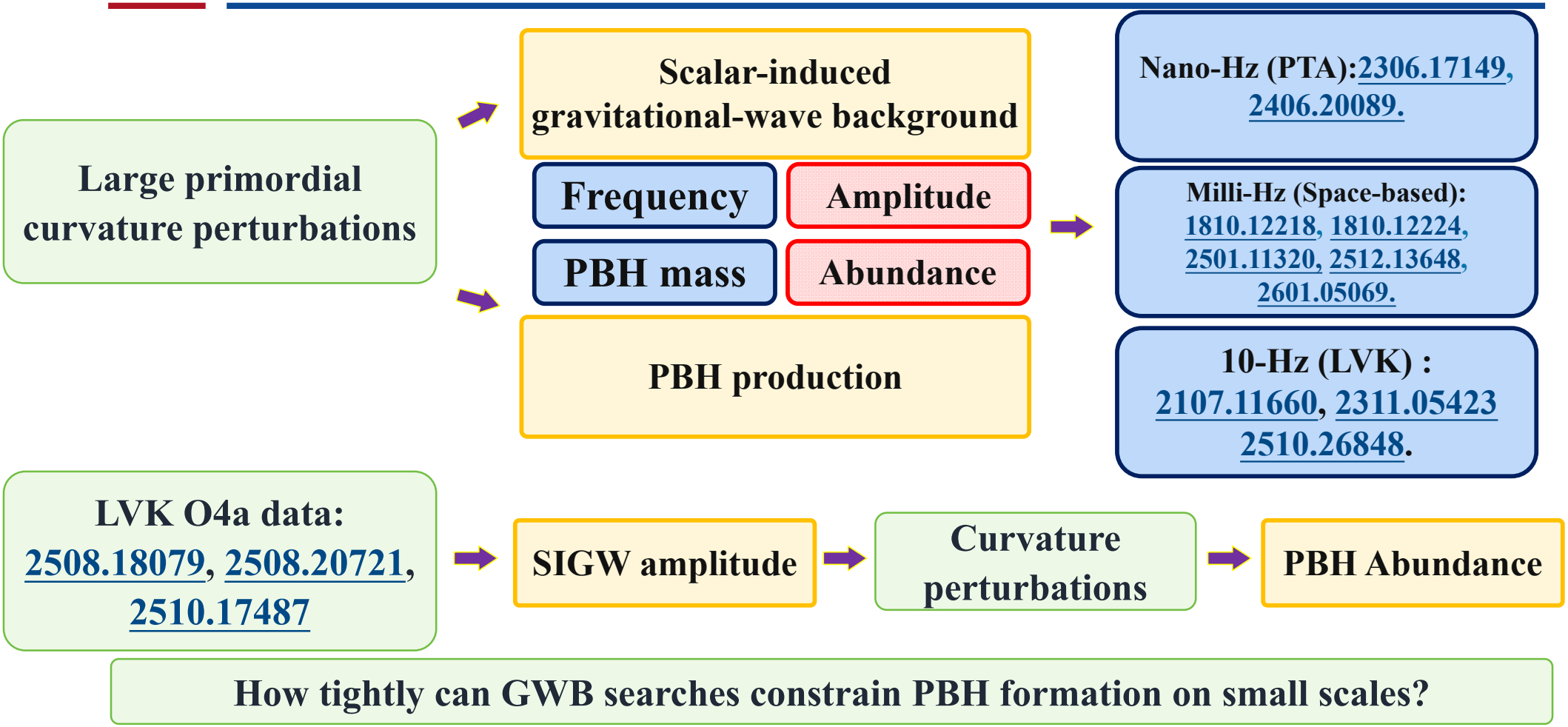
University of Chinese Academy of Sciences / ICTP-AP

with Chen Yang, Haipeng An, Huai-Ke Guo, Lian-Tao Wang and Yue Zhao

arXiv:2609.12867 ICFP 2026 · October 24th



Curvature perturbation vs SIGW and PBH



How tightly can GWB searches constrain PBH formation on small scales?

University of Chinese Academy of Sciences
ICTP-AP International Centre for Theoretical Physics Asia-Pacific 国际理论物理中心-亚太地区
qiaomai@ucas.ac.cn

Two representative inflationary scenarios

Ultra-slow roll

An exceptionally flat inflaton potential amplifies superhorizon curvature perturbations.

$$P_\zeta^{\rm USR}(f) = A_{\rm ref}\left(\frac{f}{f_{\rm ref}}\right)^4 \Theta(f_{\rm ref}-f)$$

arXiv:1811.11158 [astro-ph.CO]

Inflationary phase transition

A first-order transition in a coupled spectator sector enhances curvature perturbations through backreaction.

$\beta/H_{\rm inf}$	4	5	10	20
α_2	0.14	0.17	0.20	0.20

$$P_\zeta^{\rm InPT}(f) = A_{\rm ref}\frac{x^3}{1+(\alpha_1 x)^4+(\alpha_2 x)^9}$$

arXiv: 2009.12381, 2201.05171, 2308.00070, 2304.02361

$$x = f/f_{\rm ref}, \quad \alpha_1 = 0.31,$$

$$f_{\rm ref} = 10^{-9} e^{40-N_e}\left(\frac{H_{\rm inf}}{10^{14}\,{\rm GeV}}\right)^{1/2}\,{\rm Hz}$$

N_e counts e-folds from the **USR / InPT** epoch to the end of inflation.

Enhanced scalar perturbations source GWs at horizon reentry.

The GWB spectrum

GW energy density spectrum

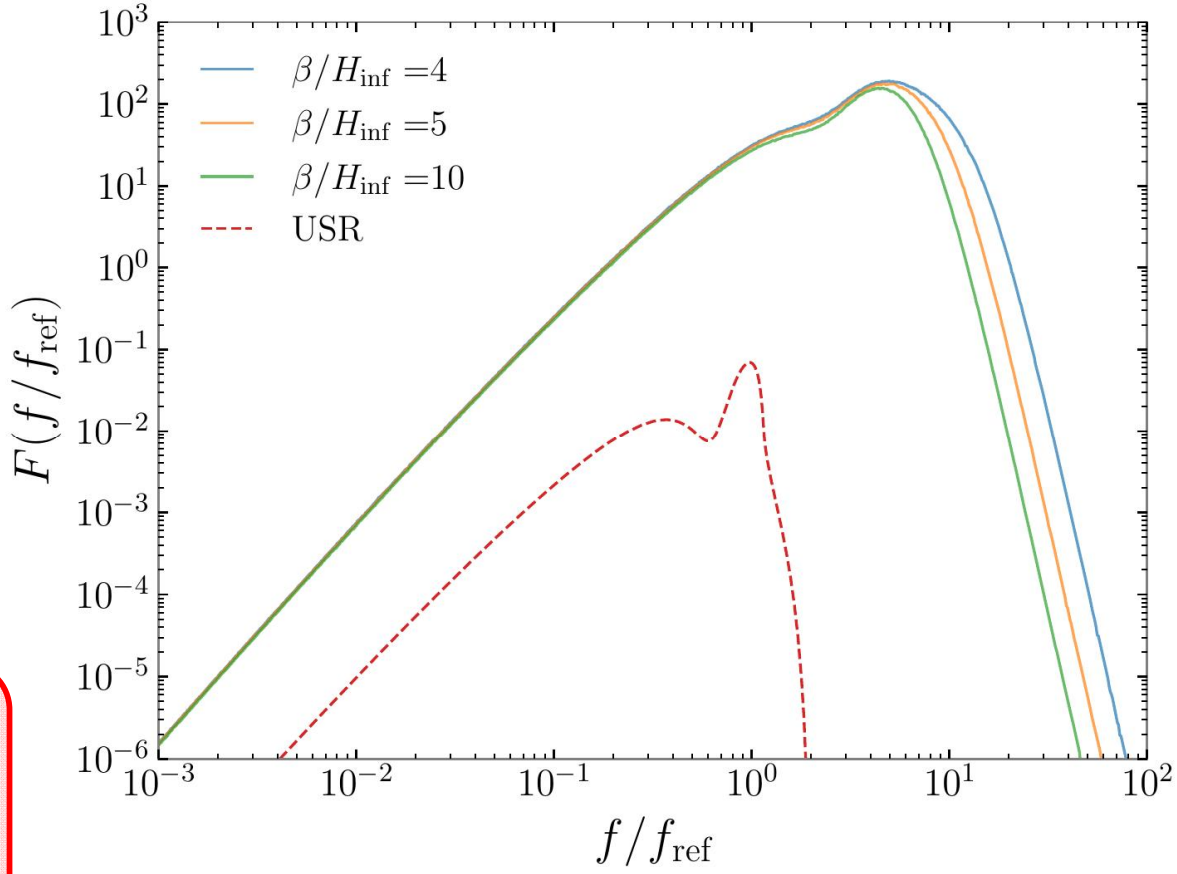
Assuming a stationary, Gaussian, non-polarized, isotropic background:

$$\Omega_{\rm GW}(f) = \frac{f}{\rho_c}\frac{d\rho_{\rm GW}}{df}$$

SIGW spectrum

$$\Omega_{\rm GW}(f) = \Omega_{\rm R} A_{\rm ref}^2 F\left(\frac{f}{f_{\rm ref}}\right)$$

$\Omega_{\rm R}$: present radiation density fraction



Mai, et. al., arXiv: 2609.12867

$A_{\rm ref}$ and $f_{\rm ref}$ can be further mapped to PBH abundance and mass, respectively.

qiaomai@ucas.ac.cn

Mapping SIGW to PBH productiom

Ultra-slow roll

$$M_{\rm PBH}^{\rm USR} = 3.1\times10^{-17} M_\odot \left(\frac{f_{\rm ref}}{\rm Hz}\right)^{-2}$$

$$f_{\rm PBH}^{\rm USR} = 5.1\times10^{16} \left(\frac{f_{\rm ref}}{\rm Hz}\right) {\rm erfc}\left(\frac{2.1}{\sqrt{A_{\rm ref}}}\right)$$

Inflationary phase transition

$$M_{\rm PBH}^{\rm InPT} = 9.7\times10^{-19} M_\odot \left(\frac{f_{\rm ref}}{\rm Hz}\right)^{-2}$$

$$f_{\rm PBH}^{\rm InPT} = 2.8\times10^{17} \left(\frac{f_{\rm ref}}{\rm Hz}\right) {\rm erfc}\left(\frac{0.26}{\sqrt{A_{\rm ref}}}\right)$$

Mai, et. al., arXiv: 2609.12867

Frequency sets the PBH mass scale. Amplitude controls the collapse probability.

Assumption:

1. Gaussian perturbations and smoothing.
2. Collapse threshold $\delta c = 0.45$.
3. Collapse efficiency $\gamma = 0.2$.
4. Monochromatic mass function at the maximum-variance scale.

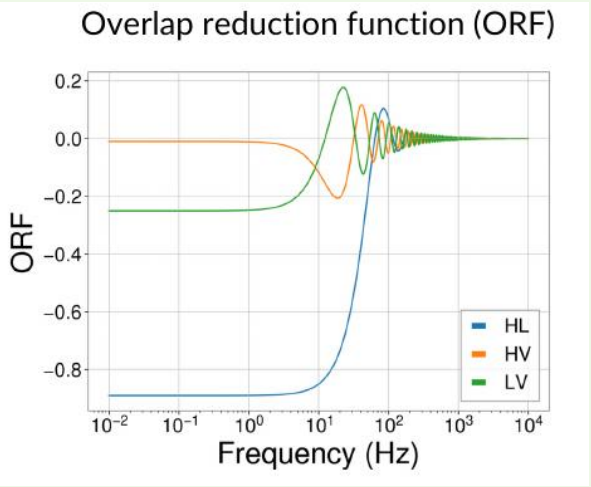
Astrophys. J. 201, 1 (1975), arXiv:2002.12778 [astroph.CO], 1801.05235 [astroph.CO], 1904.00984 [astro-ph.CO].

Cross-correlation methodology

Cross-correlation spectrum

$$\hat{C}_{IJ}(f \mid t) = \frac{2\,\mathrm{Re}[\tilde{d}_I^{\star}(f|t)\tilde{d}_J(f|t)]}{T_{\mathrm{seg}}\,\gamma_{IJ}(f)\,S_{IJ}(f)}$$

$$S_{IJ}(f) = \frac{3H_0^2 \sin\beta_I \sin\beta_J}{10\pi^2 f^3}$$



Beta IJ are Opening angles, π/2 for LVK, π/3 for ET

Variance in the weak-signal limit

$$\sigma_{IJ}^2(f \mid t) \simeq \frac{1}{2T_{\mathrm{seg}}\Delta f}\frac{P_I(f|t)P_J(f|t)}{\gamma_{IJ}^2(f)S_{IJ}^2(f)}$$

Segment length and resolution.

One-side power spectrum density (PSD).

$$\hat{C}_{IJ}(f) = \frac{\sum_t \hat{C}_{IJ}(f|t)\sigma_{IJ}^{-2}(f|t)}{\sum_t \sigma_{IJ}^{-2}(f|t)}$$

$$\sigma_{IJ}^2(f) = 1/\sum_t \sigma_{IJ}^{-2}(f|t)$$

Combine segments with inverse-variance weights.

arXiv: 2303.15696, 1201.3563

University of Chinese Academy of Sciences
ICTP-AP International Centre for Theoretical Physics Asia-Pacific 国际理论物理中心-亚太地区
qiaomai@ucas.ac.cn

Joint Bayesian inference with the CBC background

Likelihood

$$\ln \mathcal{L} = -\frac{1}{2} \sum_{IJ,k} \frac{[\hat{C}^{IJ}(f_k) - \lambda_{IJ}\Omega_{GW}(f_k)]^2}{\sigma_{IJ}^2(f_k)} + \text{const.}$$

Accounting for calibration uncertainty.

arXiv: 2303.15696

Signal model

$$\Omega_{GW}(f) = \Omega_{SIGW}(f) + \Omega_{ref}\left(\frac{f}{25\,\text{Hz}}\right)^{2/3}$$

GWB from superposition of unsolved CBC.

Log-uniform priors

Parameter	Prior Distribution
Ω_{ref}	Log10Uniform$(10^{-13}, 10^{-6})$
f_{ref} (InPT/USR)	Log10Uniform$(0.1, 10^{4})$ Hz
A_{ref} (USR)	Log10Uniform$(10^{-6}, 80)$
A_{ref} (InPT)	Log10Uniform$(10^{-8}, 10)$

Unity Omega amplitude. Ensure a conservative constraints.

Set 95% credible constraints by marginalizing CBC amplitude of the posterior.

University of Chinese Academy of Sciences
ICTP-AP International Centre for Theoretical Physics Asia-Pacific 国际理论物理中心-亚太地区
qiaomai@ucas.ac.cn

LVK O1–O4a data and data quality cut

Data

O1–O4a: LIGO Livingston, LIGO Hanford, O3: Virgo.

O4a synchronized time 126.57 days before vetoes.

192 s segments. 50% overlap.

Time-domain cut

Category 1 vetoes: time flag that detector not in a proper status.

Ensure stationary of data:

Gating:
Remove transient contamination by smoothing the glitch.

Delta sigma cut:
Remove segment variate more than 20% compared with consecutive segments

Frequency-domain cut

Notch frequency bins contaminated by known instrumental lines.

Calibration line

Quadruple suspension violin modes.

Powerline harmonics, combs, …

Projected sensitivity for future experiments

Ground: cross-correlation of detector pair IJ

$$\rho_{IJ} = \left[2T \int_{f_{\min}}^{f_{\max}} \mathrm{d}f \, \frac{S_{IJ}^2(f)\gamma_{IJ}^2(f)\Omega_{\mathrm{GW}}^2(f)}{P_{n,I}(f)P_{n,J}(f)} \right]^{1/2}$$

Total observation time

arXiv: 2609.12867, gr-qc/9710117

	A+	CE	ET	Space-based
$f_{\min}$ [Hz]	5	5	1	3×10^{-5}
$f_{\max}$ [Hz]	5×10^3	5×10^3	10^4	0.5

Space: SNR in the TDI A channel

$$\mathrm{SNR}_a^2 = 2T \int_{f_{\min}}^{f_{\max}} \left[\frac{S_A^{\mathrm{GW}}(f)}{N_A(f)} \right]^2 \mathrm{d}f$$

arXiv:2603.21762

$$S_A^{\mathrm{GW}}(f) = \frac{3H_0^2}{4\pi^2} \frac{\Omega_{\mathrm{GW}}(f)}{f^3} \mathcal{R}_A(f)$$

TDI A-channel response.

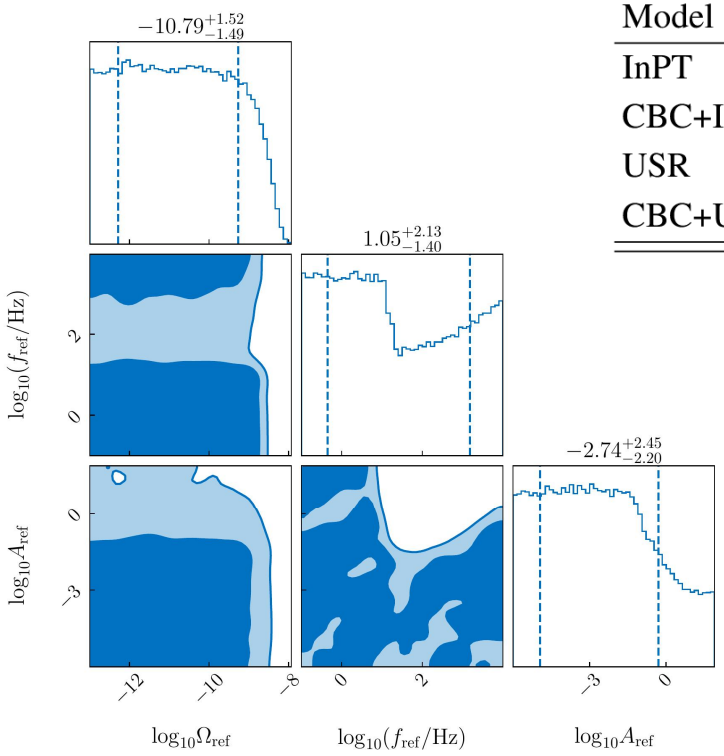
N_A: instrumental-noise PSD

Forecast contours: SNR = 2, one effective year.

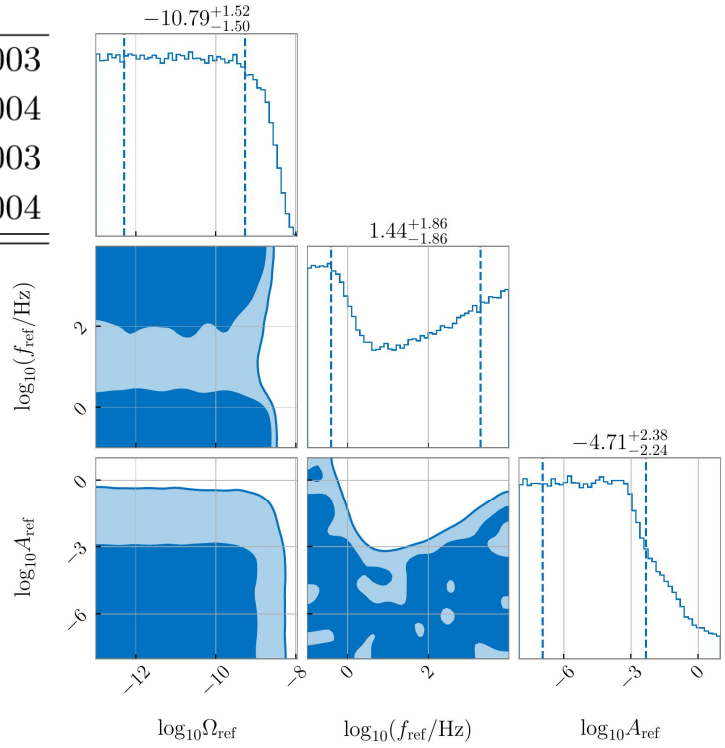
Joint posteriors with the CBC background

CBC + USR

Model	$\ln \mathcal{B}_{S/N}$
InPT	-0.315 ± 0.003
CBC+InPT	-0.780 ± 0.004
USR	-0.192 ± 0.003
CBC+USR	-0.652 ± 0.004



CBC + InPT



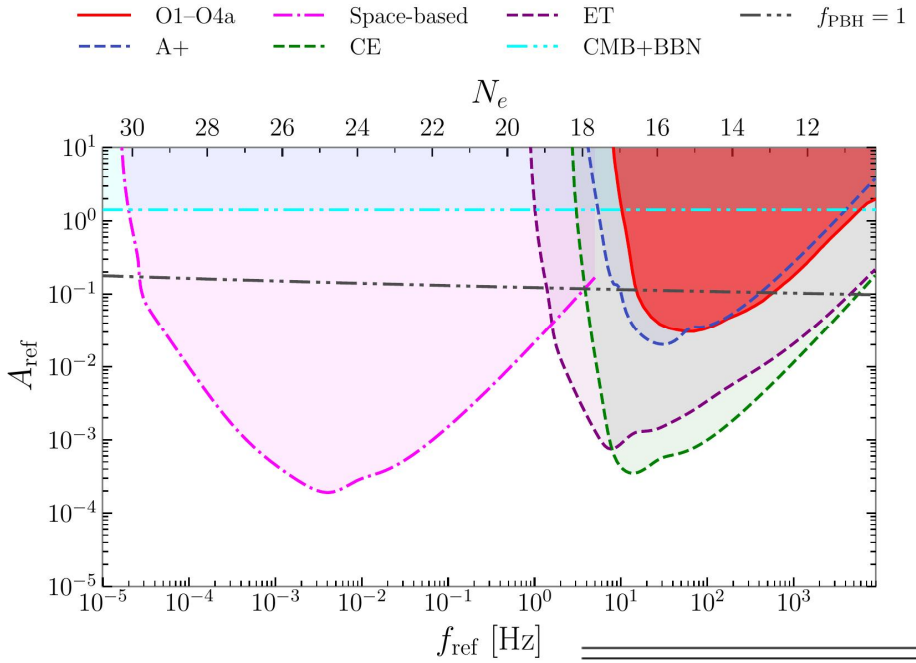
Mai, et. al., arXiv: 2609.12867

The data do not favor either signal model over noise.

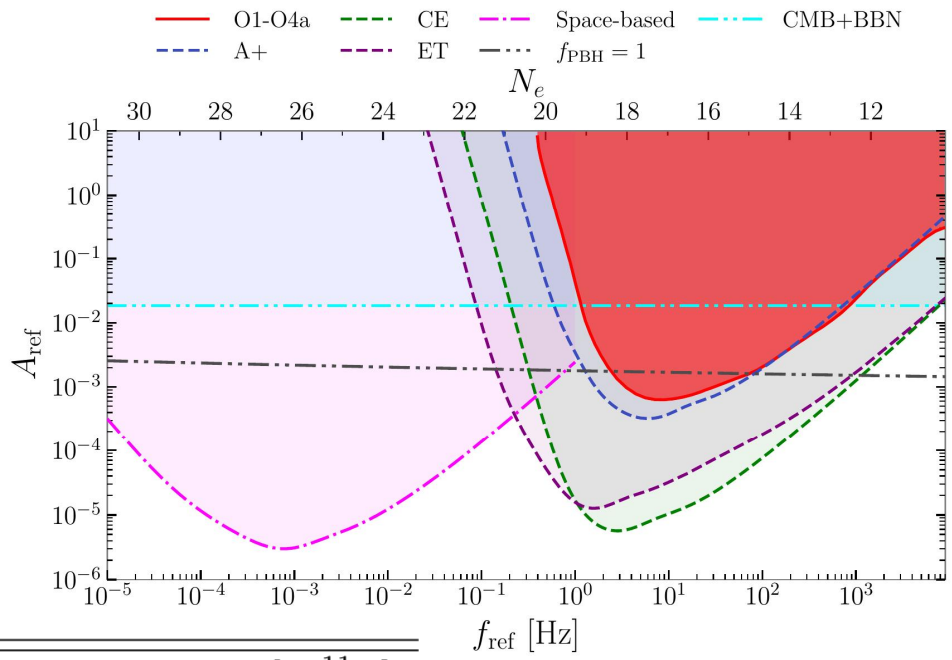
qiaomai@ucas.ac.cn

Constraints on primordial curvature perturbations

Ultra-slow roll



Inflationary phase transition



Model	$f_{\rm ref}$ [Hz]	N_e	$M_{\rm PBH}$ [10^{11} g]
USR	$(15.8,\ 562.3)$	$(12.9,\ 16.5)$	$(1.9,\ 2.5\times10^{3})$
InPT	$(2.8,\ 70.8)$	$(15.0,\ 18.2)$	$(3.8,\ 2.5\times10^{3})$

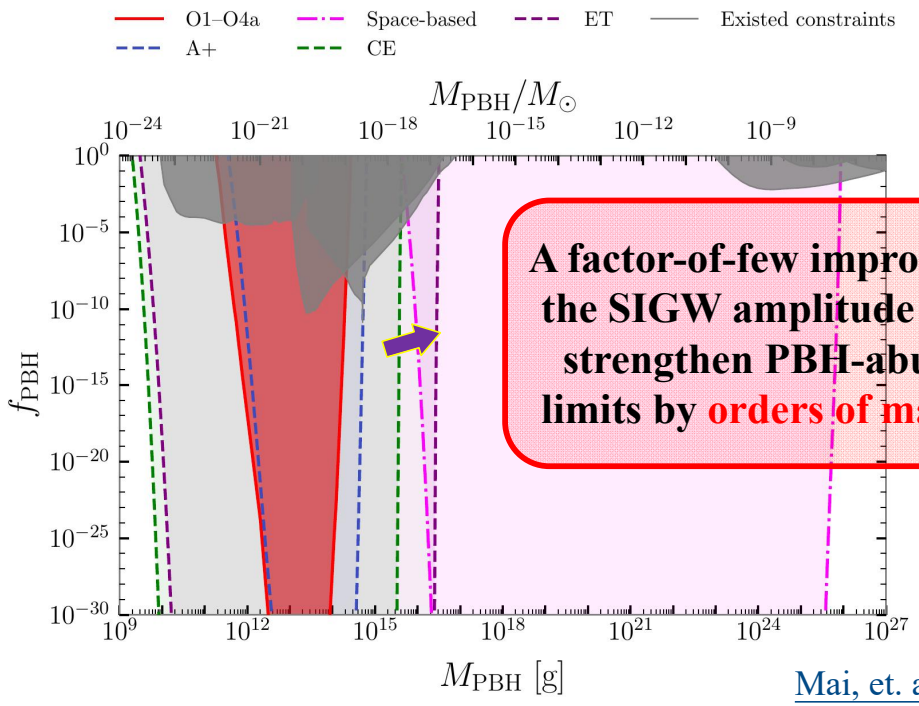
University of Chinese Academy of Sciences
ICTP-AP International Centre for Theoretical Physics Asia-Pacific 国际理论物理中心-亚太地区

Mai, et. al., arXiv: 2609.12867

qiaomai@ucas.ac.cn

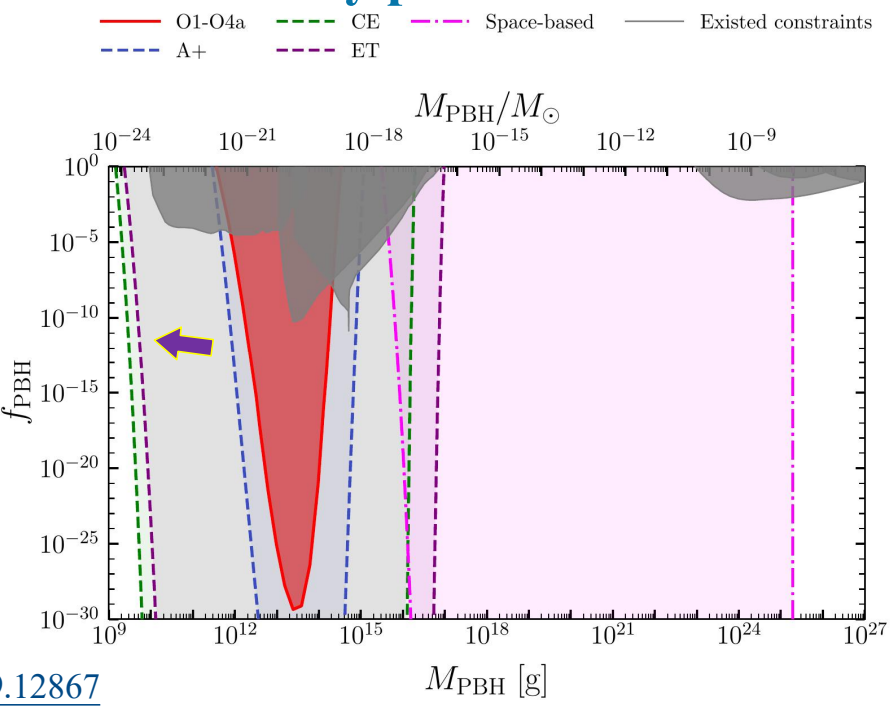
O1–O4a probes PBH abundances far below unity

Ultra-slow roll



A factor-of-few improvement in the SIGW amplitude limit can strengthen PBH-abundance limits by orders of magnitude.

Inflationary phase transition



Mai, et. al., arXiv: 2609.12867

GWB searches surpass conventional PBH limits over part of the mass range.

For evaporated PBHs, interpret these curves as constraints on formation, not a surviving population.

qiaomai@ucas.ac.cn

Conclusions

1. **No evidence** of SIGW from from two representative scenario that generates large curvature perturbation: USR and InPT.
2. 95% credible **upper limits** on SIGW **amplitude**.
3. Assuming a Gaussian perturbation and smoothing, we map the constraints on **SIGW amplitude** to **PBH abundance** and find that current SGWB searches can exceed conventional PBH limits.
4. **A factor-of-few** improvement in the scalar-amplitude limit can strengthen PBH-formation limits by **orders of magnitude** due to exponential amplitude–abundance relation.


中国科学院大学
University of Chinese Academy of Sciences
Thank you!
arXiv: 2609.12867
qiaomai@ucas.ac.cn